2021 IEEE International Conference on Pervasive Computing and Communications (PerCom) | 978-1-6654-0418-1/20/$31.00 ©2021 IEEE | DOI: 10.1109/PERCOM50583.2021.9439126

Data Collection Utility Maximization in Wireless Sensor Networks via Efficient Determination of UAV Hovering Locations

Mengyu Chen
The Australian National University
ACT, Canberra, Australia
mengyu.chen1@anu.edu.au

Weifa Liang
The Australian National University
ACT, Canberra, Australia
wliang@cs.anu.edu.au

Sajal K. Das
Missouri University of Sci. & Tech.
Rolla, Missouri, USA
sdas@mst.edu

***Abstract*—Data collection in Wireless Sensor Networks (WSNs) has been a hot research topic owing to the accelerated development in the Internet of Things (IoT). With high agility, mobility and flexibility, the Unmanned Aerial Vehicle (UAV) is widely considered as a promising technology for data collection in WSNs. Under the one-to-many data collection scheme, where a UAV is able to collect data from multiple sensors simultaneously within its reception range, the identification of hovering locations of the UAV impacts the efficiency of data collection significantly. Most existing studies either neglect this critical issue or discretize the UAV serving area into small regions with a given size, which results in the inevitable utility loss of data collection. In this paper, we jointly consider the hovering location positioning of the UAV and the utility maximization of data collection. Specifically, we first formulate a novel data collection utility maximization problem (UMP) and show that it is an NP-hard problem. We then devise an efficient algorithm for precisely positioning (potential) UAV hovering locations, which improves the data collection utility significantly. We also propose an approximation algorithm for UMP with approximation ratio $(1 - \frac{1}{e})$, where e is the base of the natural logarithm. We finally evaluate the performance of the proposed algorithms through simulation experiments, and demonstrate that the proposed algorithms significantly outperform four heuristics.**

***Index Terms*—Unmanned aerial vehicles (UAV), wireless sensor networks (WSNs), Internet of Things (IoT), data collection, approximation algorithms, utility maximization, energy efficiency.**

I. Introduction

The last decade witnessed rapid advancement of digital technology, such as the Internet of Things (IoT), having enormous applications in various domains that include wearables [1], [2], smart homes [3] and smart cities [4]–[6]. Wireless Sensor Networks (WSNs) play a central role in the context of IoT for providing a massive amount of data captured by ubiquitous sensors [7]. Thus, data collection becomes crucial to feed fresh data into IoT services while avoiding data overwritten due to limited storage capacities of IoT sensors [8]–[14]. With high agility, mobility and flexibility, the Unmanned Aerial Vehicles (UAVs) have recently received considerable attention for data collection [15]–[17]. In UAV-enabled WSNs, one or multiple UAVs fly over the network monitoring area, hover at certain locations to collect data from sensors wirelessly, and deliver the collected data to a base station for further processing [18].

In the literature, extensive efforts have been made to explore UAV-enabled WSNs in recent years. For example, in [19] the age-optimal trajectory for a UAV is studied to collect data from sensors with different priorities. The authors in [20] investigated the data collection tour for multiple UAVs to ensure data freshness. In [21] the quality of collected data is optimized by taking into account the data requirements and energy issues, where UAVs are able to wake up sensors through energy transmissions. The above works follow one-to-one data collection scheme, where data from only one sensor can be collected by the UAV at any time instant.

The advancements of wireless communication technologies have led to the emergence of one-to-many data collection scheme as a promising approach, where a UAV is able to simultaneously collect data from multiple sensors, significantly improving the data collection efficiency. For instance, in [22], optimal trajectories for multiple UAVs are developed to minimize energy consumption of IoT devices, by adopting the Orthogonal Frequency Division Multiple Access (OFDMA) technique. In [23], data collection is investigated from long-range backscatter devices via UAV, adopting the power-domain Non-Orthogonal Multiple Access (NOMA) protocol, which outperforms OFDMA in many scenarios. The authors in [24] considered the coverage problem in UAV-enabled WSNs aiming to minimize the deployment cost of UAVs, where a fleet of UAVs are deployed to continuously monitor the network and transmit the collected data to a fixed base station.

In a previous work [25], we developed an efficient approximation algorithm for the UAV data collection maximization problem under the one-to-many data collection scheme, where a set of potential hovering locations for the UAV are determined in advance. Although there exist works on data collection in UAV-enabled WSNs, it is challenging to identify the hovering locations for UAVs in the one-to-many data collection scheme. To be specific, the data collection efficiency under this scheme massively relies on the hovering locations of the UAV and the hovering duration at each such location. However, efficient determination of UAV hovering locations is widely considered to be intractable as there are infinitely many potential hovering locations in the UAV serving area.

978-1-6654-0418-1/21/$31.00 ©2021 IEEE

Authorized licensed use limited to: CITY UNIV OF HONG KONG. Downloaded on July 29,2021 at 08:11:05 UTC from IEEE Xplore. Restrictions apply.

For the sake of tractability, most of the existing approaches discretize the UAV serving area into different regions with certain sizes, where each region is regarded as a potential UAV hovering spot. However, the locations in a discretized region cannot be distinguished from each other, which results in the inevitable utility loss of data collection. Moreover, the time complexity of discretization-based approaches highly depends on the size of the network monitoring area, thus making the data collection inefficient especially for large-scale WSNs.

To address the aforementioned challenges, this paper significantly extends our previous work [25] by jointly considering the UAV hovering location positioning and the data collection utility maximization problem under the one-to-many data collection scheme, where the total hovering duration of the UAV is constrained by a given budget. Tackling this problem poses many challenges. For example, to avoid the utility loss caused by discretizations, determining precise hovering locations for the UAV from the infinitely many potential ones is non-trivial. Moreover, jointly considering the hovering location determination and the data collection utility, while separating the computational complexity from the network size, makes the problem further complex. Finally, the allocation of UAV hovering time budget at each selected hovering location also impacts the data collection utility significantly.

To the best of our knowledge, we are the first to focus on enhancing UAV hovering location positioning to improve data collection utility in WSNs. To this end, we propose an efficient algorithm to precisely identify a finite set of potential hovering locations for the UAV from the infinitely many ones, which significantly improves the data collection utility as compared with four baseline heuristics.

The main contributions of this paper are summarized below.

- We formulate a novel data collection Utility Maximization Problem (UMP) to maximize the utility of data collection under the one-to-many data collection scheme. We also show that the problem is NP-hard.
- We devise an efficient algorithm to precisely determine the UAV's potential hovering locations, thus improving the data collection utility significantly, where we jointly consider the UAV hovering location positioning and data collection utility maximization.
- We devise an approximation algorithm for UMP with approximation ratio $(1 - \frac{1}{e})$ for the problem, where e is the base of the natural logarithm.
- We evaluate the performance of the proposed algorithms through extensive simulation experiments, demonstrating the superiority of the proposed algorithms.

The rest of the paper is organized as follows. Section II introduces the system model, data collection tour model, data collection utility model, and the problem definition. Section III studies the defined problem and designs an approximation algorithm. Section IV analyzes the approximation ratio of the proposed algorithm. Section V reports the performance results of the proposed algorithms via simulation study. Section VI concludes the paper.

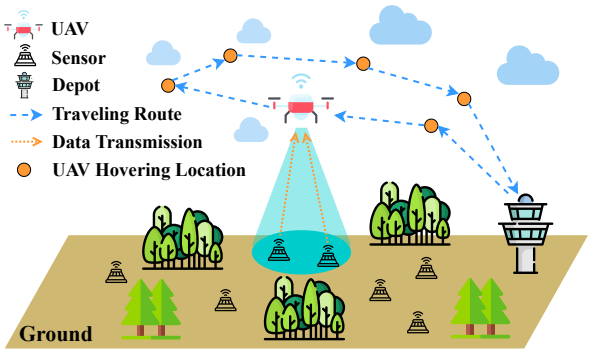

Fig. 1: An illustrative example of data collection in a UAV-enabled WSN.

II. Preliminaries

In this section, we first introduce various models such as the system model, and data collection tour and utility models. We then formulate the data collection utility maximization problem in WSNs and show that it is NP-hard.

A. System Model

We consider a wireless sensor network (WSN) serving a two-dimensional region of length $\mathcal{L}$ and width $\mathcal{W}$. A set $\mathcal{V} = \{v_i \mid 1 \leq i \leq N\}$ of homogeneous sensors are deployed in the region, where each sensor v_i has a unique location, denoted by $(x_i, y_i, 0)$. Assume the sensors perform environmental monitoring continuously, acquire and store a huge amount of data. Let D_i denote the volume of data at sensor $v_i \in \mathcal{V}$.

To avoid data loss or being overwritten at each sensor, a UAV is dispatched periodically for data collection from the sensors. The UAV departs from a depot, hovers on certain locations to collect data from the sensors, and then delivers the collected data to a data center for further processing. Fig. 1 shows an illustrative example. For safety considerations imposed by regulatory authorities, the UAV is assumed to travel at a fixed altitude H above the ground [15]. In this paper, we assume that the depot is co-located with the data center, unless otherwise stated.

Supported by the OFDMA technique, the UAV is able to collect data simultaneously from multiple sensors, whose Euclidean distance from the UAV is no larger than R, with a data transmission bandwidth B from each sensor.

B. Data Collection Tour Model

A *data collection tour* of the UAV is a closed tour starting from and ending at the depot. The tour is a sequence of hovering locations, at altitude H, which the UAV visits one after another for data collection. Since there are infinitely many locations at altitude H, an important challenge for scheduling the data collection tour is to identify a sequence of UAV's hovering locations that improves efficiency of data collection.

Let $\mathcal{H}$ denote a sequence of selected hovering locations for the UAV on a data collection tour, i.e.,

$$\mathcal{H} = (h_1,\ h_2,\ \ldots,\ h_k,\ \ldots,\ h_K), \tag{1}$$

Authorized licensed use limited to: CITY UNIV OF HONG KONG. Downloaded on July 29,2021 at 08:11:05 UTC from IEEE Xplore. Restrictions apply.

where h_k presents the kth hovering location, and K denotes the total number of selected hovering locations on the tour. Under the one-to-many data collection scheme, when hovering at $h_k = (X_k, Y_k, H)$, the UAV is able to collect data from a subset of sensors whose Euclidean distance from the UAV is no greater than a given value R. Let us define the *data collection sensor set*, S_k, as the set of sensors whose data can be collected when the UAV hovers at location h_k, i.e.,

$$S_k = \{v_i \mid (x_i - X_k)^2 + (y_i - Y_k)^2 + H^2 \leq R^2,\ v_i \in \mathcal{V}\}. \tag{2}$$

Correspondingly, the data from a sensor v_i can be collected multiple times when the UAV sojourns at different hovering locations of $\mathcal{H}$. Let L_i denote the set of hovering locations of $\mathcal{H}$ which are within the data transmission range of v_i, i.e.,

$$L_i = \{h_k \mid (x_i - X_k)^2 + (y_i - Y_k)^2 + H^2 \leq R^2, \\ 1 \leq k \leq K\}. \tag{3}$$

Given the sequence $\mathcal{H}$ of selected hovering locations, the duration T_k for which the UAV sojourns at location h_k is also crucial for the data collection performance. We define the sequence $\mathcal{T}$ of hovering duration corresponding to $\mathcal{H}$ as

$$\mathcal{T} = (T_1,\ T_2,\ \ldots,\ T_k,\ \ldots,\ T_K). \tag{4}$$

C. Data Collection Utility Model

Constrained by its energy capacity, the UAV is unlikely to collect data from all sensors in one tour for a large-scale WSN, it is expected that the UAV is capable to collect data from sensors in important regions in the monitoring area. We consider spatial-temporal correlations among sensors, and model the data collection utility from each sensor by a submodular *utility function*.

Denote by $F_i(t)$ the *utility function* of sensor v_i, which represents the accumulative utility obtained by the UAV when hovering within the data transmission range of v_i for t time units. Denote by $t_i^{max} = \frac{D_i}{B}$ the number of time units required for collecting all data from v_i, where D_i and B are respectively the volume of data at v_i and the data transmission bandwidth. Without loss of generality, we assume that t_i^{max} is an integer. It can be seen that the accumulative utility obtained from v_i increases with the growth of t from 0 to t_i^{max}, and maintains at $F_i(t_i^{max})$ when t is greater than t_i^{max}.

Definition 1: The defined utility function $F_i(t)$ has the following properties.

1) $F_i(t) = 0$ if $t = 0$; $F_i(t) > 0$ if $0 < t \leq t_i^{max}$; otherwise $F_i(t) = F_i(t_i^{max})$ if $t > t_i^{max}$, where $t \in \mathbb{N}$.
2) $F_i(t)$ is a non-decreasing function, i.e., $F_i(t_1) \leq F_i(t_2)$ for $0 \leq t_1 < t_2$, where $t_1,\ t_2 \in \mathbb{N}$.
3) $F_i(t)$ is a submodular function, where $F_i(t_1 + \Delta) - F_i(t_1) > F_i(t_2 + \Delta) - F_i(t_2)$ for $0 \leq t_1 < t_2 \leq t_i^{max}$ and $F_i(t_1 + \Delta) - F_i(t_1) = F_i(t_2 + \Delta) - F_i(t_2)$ for $t_i^{max} \leq t_1 < t_2$, where $t_1 \in \mathbb{N}$ and $t_2,\ \Delta \in \mathbb{N}^+$.

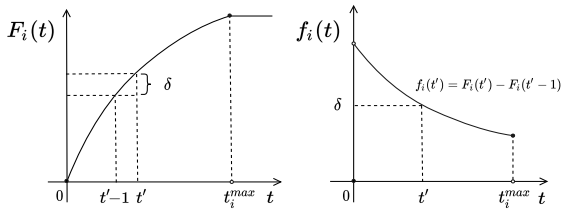

Fig. 2: An example of utility function $F_i(t)$ and utility margin function $f_i(t)$, where $F_i(t') - F_i(t'-1) = \delta$ and $f_i(t') = \delta$.

To model the utility gain at time unit t when the UAV collects data from a sensor v_i, the *utility margin function* $f_i(t)$ is defined as follows.

$$f_i(t) = \begin{cases} F_i(t) - F_i(t-1), & \text{if } t \in \mathbb{N}^+, \\ 0, & \text{if } t = 0. \end{cases} \tag{5}$$

Definition 2: The defined utility margin function $f_i(t)$ has the following properties.

1) $f_i(t_1) > f_i(t_2)$ for $1 \leq t_1 < t_2 \leq t_i^{max}$ and $t_1,\ t_2 \in \mathbb{N}^+$.
2) $f_i(t) = 0$ for any $t > t_i^{max}$ and $t \in \mathbb{N}^+$.

Fig. 2 is an illustrative example of the utility margin function $f_i(t)$ from the utility function $F_i(t)$.

We define u_i as the sum of utility obtained from a sensor v_i during a tour, which is associated with the accumulative duration when the UAV hovers at locations in L_i, i.e.,

$$u_i = F_i(\sum_{h_k \in L_i} T_k), \tag{6}$$

recalling that L_i is the set of hovering locations of $\mathcal{H}$ within the data transmission range of v_i, as defined in Eq. (3), T_k is the accumulative hovering duration at location h_k.

Denote by U the total data collection utility of a tour, which can be calculated by accumulating the utility u_i obtained from each sensor $v_i \in \mathcal{V}$, i.e.,

$$U = \sum_{v_i \in \mathcal{V}} u_i. \tag{7}$$

D. Data Collection Utility Maximization Problem

We formulate a novel *data collection utility maximization problem* (UMP) in WSNs as follows.

Consider a WSN with a set $\mathcal{V} = \{v_i \mid 1 \leq i \leq N\}$ of sensors deployed in a $\mathcal{L} \times \mathcal{W}$ region. Each sensor $v_i \in \mathcal{V}$ has a data transmission bandwidth B and data transmission range R, with a volume D_i of data to be collected. We assume the utility function $F_i(t)$ of each sensor v_i is pre-defined. A UAV with hovering duration budget Γ travels at a fixed altitude H above the WSN for data collection. Then the UMP is to find a closed data collection tour for the UAV (starting and ending at the depot), which consists of a sequence of hovering locations and hovering duration at each such one, aiming at maximizing the total utility of data collected from the sensors in the WSN.

Authorized licensed use limited to: CITY UNIV OF HONG KONG. Downloaded on July 29,2021 at 08:11:05 UTC from IEEE Xplore. Restrictions apply.

Formally the problem UMP is formulated as:

$$\text{Maximize} \quad U, \tag{8}$$

$$\text{subject to} \quad h_k = (X_k, Y_k, H), \qquad \forall 1 \le k \le K \tag{9}$$

$$-R \le X_k \le \mathcal{L} + R, \qquad \forall 1 \le k \le K \tag{10}$$

$$-R \le Y_k \le \mathcal{W} + R, \qquad \forall 1 \le k \le K \tag{11}$$

$$T_k \in \mathbb{N}^+, \qquad \forall 1 \le k \le K \tag{12}$$

$$\sum_{k=1}^{K} T_k \le \Gamma, \tag{13}$$

Constraints (10) and (11) are used to bound the serving area of the UAV, and assume that the depot is located within the UAV serving area. Constraint (13) limits the total hovering duration of the UAV to be no greater than the given hovering budget Γ.

E. NP Hardness of UMP

Theorem 1: The data collection utility maximization problem (UMP) is NP-hard.

Proof We show the NP-hardness of UMP by a reduction from an NP-hard problem – the Robust K-Center problem (RKC) [26]. Given a set V of points in a 2-D plane and K disks with radii r, the decision version of the RKC is to cover at least $M \le |V|$ points by the disks, where M is a given integer. This problem has been shown to be NP-hard [27].

Let I and I_U be the instances of RKC and UMP, respectively. We show that I can be reduced to I_U in polynomial time as follows.

The number K of disks in I corresponds to the number Γ of UAV hovering time units in I_U, i.e., $K = \Gamma$. Denote by V_I the point set in I, which corresponds to the sensor set $\mathcal{V}_U$ in I_U, where there is a corresponding sensor $v_i \in \mathcal{V}_U$ at location $(a_i, b_i, 0)$ of each point with coordinates (a_i, b_i) in I with $1 \le i \le |V|$.

For each disk k with $1 \le k \le K$, there is a corresponding hovering location h_k for the UAV. When the UAV hovers at location h_k, it can collect all data from sensors in S_k within one time unit, assuming that the data volume D_i of each sensor $v_i \in \mathcal{V}_U$ is B, where B is the data transmission bandwidth of v_i. Also, the utility of each sensor v_i is identical by setting $F_i(0) = 0$ and $F_i(t) = 1$ if $t \ge 1$ at each time unit t. The data transmission range of each sensor is $R = \sqrt{H^2 + r^2}$, where r is the radius of each disk in I, and H is the hovering altitude of the UAV in I_U.

Following the reduction from I to I_U, each sensor has an identical utility function with identical volume B of data to be collected, the data of all sensors in S_k can be collected by the UAV at location h_k within one time unit. Also, the accumulative utility obtained at time unit k is determined by the number of sensors in S_k whose data have not been collected yet. Hence, maximizing the data collection utility of I_U is equivalent to covering the maximum number of points in I by the K disks with $K = \Gamma$.

Denote by OPT and $|OPT|$ an optimal solution of I_U and the value of OPT, respectively. A solution for I then can be derived from the solution OPT. Recall that M is the minimum number of points required to be covered in I. If $|OPT| < M$, the maximum number of sensors covered by the K disks is less than M, and there is no feasible solution for I. Otherwise, for the hovering location sequence $\mathcal{H}$ of OPT with $|\mathcal{H}| = K$, we can generate a set of points in I, where for each hovering location (X_j, Y_j, H) of $\mathcal{H}$, there is a corresponding point (X_j, Y_j) on the 2-D plane to the point set that consists of disk locations, which is a feasible solution for I. Thus a feasible solution to I_U in turn returns a feasible solution to I, and the reduction is in polynomial time. The theorem then follows. □

III. Approximation Algorithm for Data Collection Utility Maximization Problem

In this section, we study the data collection utility maximization problem (UMP) by proposing an approximation algorithm.

A. Overview of the Approximation Algorithm

Given the budget of Γ hovering time units, the UMP is to find a closed data collection tour for the UAV containing a sequence of hovering locations, each with a hovering duration, aiming at maximizing the total data collection utility.

The hovering location identification for the UAV is quite challenging since it is impossible to examine every location over the UAV serving area (with infinitely many locations). To tackle this problem, we narrow down the UAV serving area to a finite $\mathbb{M}$-Set, which always contains a location q_t^*, for any time unit t, with the global[1] maximum utility gain. From the identified $\mathbb{M}$-Set, q_t^* is iteratively selected at each time unit t, for $1 \le t \le \Gamma$; it is possible that a location is chosen within multiple iterations, i.e., $q_a^* = q_b^*$ where $a \ne b$. Consequently, a sequence L of locations are obtained after Γ iterations. We then regard each distinct location $l \in L$ as a hovering location for the UAV and recognize the number of replications of l contained in L as the hovering duration at l. Finally, a data collection tour is obtained by forming a closed circuit visiting the selected hovering locations and the depot, with the corresponding hovering duration. The proposed algorithm for the UMP is an approximation algorithm with a provable approximation ratio of $(1 - \frac{1}{e})$.

B. Potential Hovering Location Set: $\mathbb{M}$-Set

In the following, we propose to narrow down the UAV serving area to a finite '$\mathbb{M}$-Set' for further processing.

Definition 3: A potential hovering location set $\mathcal{M}$ is recognized as an $\mathbb{M}$-Set if it has the following two properties:

1) $\mathcal{M}$ is a finite hovering location set.
2) There always exists a location $q_t^* \in \mathcal{M}$, where the utility gain at q_t^* at time unit t is no less than the utility gain at any other location in the UAV serving area at time unit t, for $1 \le t \le \Gamma$.

[1]The utility gain for any location q in the UAV serving area is no greater than the utility gain at q_t^* at time unit t.

Authorized licensed use limited to: CITY UNIV OF HONG KONG. Downloaded on July 29,2021 at 08:11:05 UTC from IEEE Xplore. Restrictions apply.

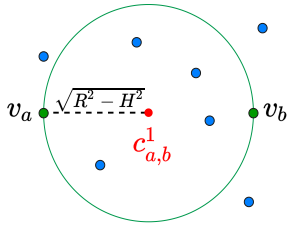

Fig. 3: Only $O^1_{a,b}$ exists if $|v_a v_b| = 2\sqrt{R^2-H^2}$, with the center $c^1_{a,b} = (\frac{x_a+x_b}{2}, \frac{y_a+y_b}{2}, 0)$.

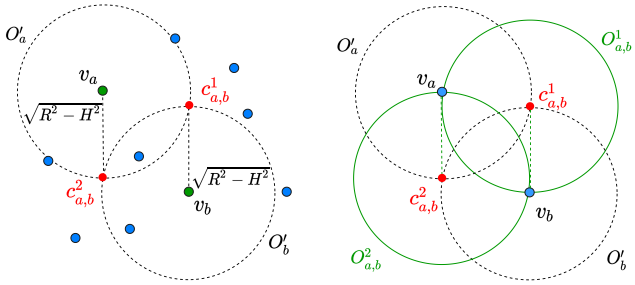

Fig. 4: An illustrative example to identify $O^1_{a,b}$ and $O^2_{a,b}$ if $0 < |v_a v_b| < 2\sqrt{R^2-H^2}$. (a) Form O'_a and O'_b with radius $\sqrt{R^2-H^2}$ centered at v_a and v_b respectively, where $c^1_{a,b}$ and $c^2_{a,b}$ are the intersection points. (b) Centered at $c^1_{a,b}$ and $c^2_{a,b}$ respectively, $O^1_{a,b}$ and $O^2_{a,b}$ are obtained with radius $\sqrt{R^2-H^2}$, covering both v_a and v_b on their circumferences.

By utilizing an $\mathbb{M}$-Set, we can identify q^*_t by finding a location with the largest utility gain in $\mathcal{M}$ at time unit t. In the following, we develop an algorithm to identify an $\mathbb{M}$-Set.

Let (v_a, v_b) be a pair of sensors, where sensors $v_a \in \mathcal{V}$ and $v_b \in \mathcal{V}$ have coordinates $(x_a, y_a, 0)$ and $(x_b, y_b, 0)$, respectively. Denote by $O^s_{a,b}$ such a circle on the ground with a fixed radius $\sqrt{R^2-H^2}$ that both v_a and v_b are on its circumference with $s \in \{1, 2\}$, and denote by $|v_a v_b|$ the Euclidean distance between v_a and v_b. Then, a pair of sensors can be classified into three cases as follows.

- **Case 1:** $|v_a v_b| > 2\sqrt{R^2-H^2}$, $O^s_{a,b}$ does not exist.
- **Case 2:** $|v_a v_b| = 2\sqrt{R^2-H^2}$**.** As illustrated in Fig. 3, only $O^1_{a,b}$ exists and v_a and v_b on the circumference of the circle. The center of $O^1_{a,b}$ is $c^1_{a,b} = (\frac{x_a+x_b}{2}, \frac{y_a+y_b}{2}, 0)$.
- **Case 3:** $0 < |v_a v_b| < 2\sqrt{R^2-H^2}$**.** There are two circles $O^1_{a,b}$ and $O^2_{a,b}$ and v_a and v_b are on their circumferences. To obtain $O^1_{a,b}$ and $O^2_{a,b}$, we first form two auxiliary circles O'_a and O'_b centered at v_a and v_b with radius $\sqrt{R^2-H^2}$ respectively. Denote by $c^1_{a,b}$ and $c^2_{a,b}$ the intersection points of O'_a and O'_b. We can then identify $O^1_{a,b}$ and $O^2_{a,b}$ with radius $\sqrt{R^2-H^2}$ centering at $c^1_{a,b}$ and $c^2_{a,b}$ respectively. As a result, both v_a and v_b will be on the circumferences of $O^1_{a,b}$ and $O^2_{a,b}$. Fig. 4 presents an illustrative example.
  The coordinates of $c^1_{a,b}$ and $c^2_{a,b}$ can be obtained through solving the following equations.

$$\begin{cases} (X_{a,b}-x_a)^2 + (Y_{a,b}-y_a)^2 = R^2 - H^2, \\ (X_{a,b}-x_b)^2 + (Y_{a,b}-y_b)^2 = R^2 - H^2. \end{cases} \tag{14}$$

  Let $(X^1_{a,b}, Y^1_{a,b})$ and $(X^2_{a,b}, Y^2_{a,b})$ be the solutions of Eqs.(14). We then have $c^1_{a,b} = (X^1_{a,b}, Y^1_{a,b}, 0)$ and $c^2_{a,b} = (X^2_{a,b}, Y^2_{a,b}, 0)$.

Following the discussion of the three cases, $O^s_{a,b}$ (if exists) centered at $c^s_{a,b}$ for each pair of sensors v_a and v_b can be found. The projection of $c^s_{a,b}$ at altitude H then can be added to the $\mathbb{M}$-Set $\mathcal{M}$ as a potential hovering location for the UAV. Furthermore, the projection (x_i, y_i, H) of the coordinates of each sensor v_i at altitude H is also added to $\mathcal{M}$.

The detailed algorithm for identifying an $\mathbb{M}$-Set is presented in `Algorithm 1`.

Algorithm 1 Algorithm for identifying an $\mathbb{M}$-Set

Input: A set $\mathcal{V}$ of sensors, data transmission range R of sensors, hovering altitude H of the UAV.
Output: An $\mathbb{M}$-Set;

```
M ← ∅;
r ← √(R² − H²);
for each sensor v_i ∈ V do
    M ← M ∪ {(x_i, y_i, H)};
for each sensor pair (v_a, v_b) do
    if |v_a v_b| = 2r then
        M ← M ∪ {((x_a+x_b)/2, (y_a+y_b)/2, H)};
    else if |v_a v_b| < 2r then
        Find the solutions (X_1^{a,b}, Y_1^{a,b}), (X_2^{a,b}, Y_2^{a,b}) of Eqs. (14);
        M ← M ∪ {(X_1^{a,b}, Y_1^{a,b}, H), (X_2^{a,b}, Y_2^{a,b}, H)};
return M
```

C. Approximation Algorithm

Inspired by our previous work [25], let us now develop an approximation algorithm for UMP with a provable $(1-\frac{1}{e})$ ratio by utilizing the $\mathbb{M}$-Set and the defined utility function.

Let L denote a sequence of locations selected for each time unit, i.e.,

$$L = < l_1,\ l_2,\ ...,\ l_t,\ ...,\ l_{\Gamma-1},\ l_\Gamma >, \tag{15}$$

where l_t is the selected location at time unit t with $1 \le t \le \Gamma$.

Due to overlapping between covered sensors of different hovering locations, the data collection utility gain at a location m_j at time unit t is determined by all locations $l_1, l_2, ..., l_{t-1}$ selected so far. Fig. 5 provides an illustrative example. For the sake of convenience, we just assume the utility margin function $f_i(t)$ of each sensor appeared on this diagram is $f_i(1) = 1$ and $f_i(t) = 0$ for $t \ge 2$. The utility gain at p_2 for the second time unit is $f_5(1) + f_6(1) = 2$, if p_1 is selected for the first time unit; whereas it is $f_2(1) + f_3(1) + f_4(1) + f_5(1) = 4$ if p_3 is selected for the first time unit. To figure out the utility gain at a location m_j and at time unit t, we thus have to focus on the remaining data at each sensor covered by m_j.

Authorized licensed use limited to: CITY UNIV OF HONG KONG. Downloaded on July 29,2021 at 08:11:05 UTC from IEEE Xplore. Restrictions apply.

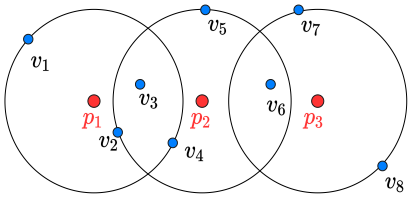

Fig. 5: An example of the utility gain at a location at a certain time unit affected by the selected locations so far.

Denote by T_i^t the number of locations within the transmission range of v_i contained in the subsequence of selected locations $< l_1, l_2, \ldots, l_t >$, where $T_i^0 = 0$. Once the hovering location l_{t+1} is identified, the corresponding hovering duration T_i^{t+1} is determined as:

$$T_i^{t+1} = \begin{cases} T_i^t + 1, & \text{if } l_{t+1} \in L_i, \\ T_i^t, & \text{otherwise}, \end{cases} \tag{16}$$

where $l_{t+1} \in L_i$ indicates that the selected location l_{t+1} is within the data transmission range of sensor v_i.

We then obtain the utility gain at a hovering location m_j for a certain time unit t by aggregating the utility gain $f_i(T_i^{t-1} + 1)$ at each sensor $v_i \in S_j$, where $f_i(t)$ is the utility margin function at v_i defined in Eq. (5). Recall that S_j is the set of sensors covered by hovering location m_j defined in Eq.(2). Denote by $\Lambda_j(t)$ the utility gain at hovering location m_j at time unit t, where $1 \leq t \leq \Gamma$. Thus,

$$\Lambda_j(t) = \sum_{v_i \in S_j} f_i(T_i^{t-1} + 1). \tag{17}$$

Having the set $\mathbb{M}$-Set $\mathcal{M}$ and the utility gain $\Lambda_j(t)$ at each location $m_j \in \mathcal{M}$, the proposed algorithm for UMP proceeds as follows.

Initialization. $T_i^0 = 0$ for any sensor $v_i \in \mathcal{V}$.

Identification of the location sequence L. For each t with $1 \leq t \leq \Gamma$, we iteratively select a location $l_t = m_{j^*}$ with the maximum $\Lambda_{j^*}(t)$ from the $\mathbb{M}$-Set $\mathcal{M}$ according to Eq. (17), and obtain T_i^t for each $v_i \in \mathcal{V}$ by Eq. (16). Consequently, a hovering location sequence L defined in Eq. (15) is obtained.

Extraction of hovering duration. Each distinct location in L is a hovering location of the UAV. Note that, there could be multiple duplicates of a hovering location in L, and the number of duplicates of a location m_j is counted as the hovering duration at m_j. For instance, for the case where $L =< p_1, p_4, p_1, p_2, p_1, p_4 >$ with $\Gamma = 6$, the hovering locations for the UAV are p_1, p_2 and p_4 with hovering duration 3, 1 and 2 time units, respectively.

Data collection tour scheduling. With the hovering locations extracted from L, a data collection tour is generated by forming a closed circuit visiting each selected hovering location including the depot, with corresponding hovering duration identified by the previous step.

Algorithm 2 Algorithm for the UMP

Input: A set $\mathcal{V}$ of sensors, data transmission range R of sensors, hovering altitude H of the UAV, the maximum number Γ of hovering time units of the UAV per tour.
Output: A data collection tour $\mathcal{C}$ for the UAV;

An $\mathbb{M}$-Set $\mathcal{M}$ is delivered by calling `Algorithm 1`;
S_j is derived for each location $m_j \in \mathcal{M}$;
$E \leftarrow \{E_j = 0 \mid m_j \in \mathcal{M}\}$; /*$E_j$ is hovering duration at m_j*/
$T \leftarrow \{T_i^t = 0 \mid 0 \leq t \leq \Gamma,\ v_i \in \mathcal{V}\}$;
for $t \leftarrow 1$ to Γ **do**
    Identify an index j^* such that $j^* \leftarrow \text{argmax}_{m_j \in \mathcal{M}} \Lambda_j(t)$ by Eq. (17);
    $E_{j^*} \leftarrow E_{j^*} + 1$;
    for each $v_i \in \mathcal{V}$ **do**
        if $v_i \in S_{j^*}$ **then**
            $T_i^t \leftarrow T_i^{t-1} + 1$;
        else
            $T_i^t \leftarrow T_i^{t-1}$;
for each $m_j \in \mathcal{M}$ **do**
    if $E_j \geq 1$ **then**
        $\mathcal{F} \leftarrow \mathcal{F} \cup \{(m_j, E_j)\}$;
    Find a closed tour $\mathcal{C}$ containing the depot and each location m_j in $\mathcal{F}$, where E_j is the hovering duration when the UAV sojourns at m_j for data collection;
return $\mathcal{C}$

IV. Algorithm Analysis

In this section, we first show that the hovering location set $\mathcal{M}$ delivered by `Algorithm 1` is consistent with the properties of $\mathbb{M}$-Set in Definition 3. Then we show that the approximation ratio of `Algorithm 2` is $(1 - \frac{1}{e})$, where e is the base of natural logarithm.

Denote by $\mathcal{M}_1$ and $\mathcal{M}_2$ the subsets of locations identified from sensor locations (Step 3 and Step 4 of `Algorithm 1`) and sensor pairs (from Step 5 to Step 10 of `Algorithm 1`), respectively. We consider the utility gain at time unit t, where locations $l_1, l_2, \ldots, l_{t-1}$ for the first $(t-1)$ time units have been identified already. Denote by p_{max} the location with the maximum utility gain Λ_{max} over the UAV serving area at time unit t, which is not necessarily contained in $\mathcal{M}$. Denote by S_{max} the data collection sensor set of p_{max}. To show that there exists a location $m \in \mathcal{M}$ with the same utility gain $\Lambda_m = \Lambda_{max}$ at time unit t, we consider $|S_{max}| = 1$ and $|S_{max}| \geq 2$ respectively.

Lemma 1: If $|S_{max}| = 1$, there exists a location $m \in \mathcal{M}_1$ with the utility gain $\Lambda_m = \Lambda_{max}$ at time unit t.

Proof Denote by v_{max} the only sensor in S_{max} with location $(x_{max}, y_{max}, 0)$, i.e., $S_{max} = \{v_{max}\}$. In `Algorithm 1`, $m = (x_{max}, y_{max}, H)$ is an element in $\mathcal{M}_1$ according to Step 3 and Step 4. Letting S_m denote the data collection sensor set of m, clearly $v_{max} \in S_m$. Thus $S_{max} \subseteq S_m$ with

Authorized licensed use limited to: CITY UNIV OF HONG KONG. Downloaded on July 29,2021 at 08:11:05 UTC from IEEE Xplore. Restrictions apply.

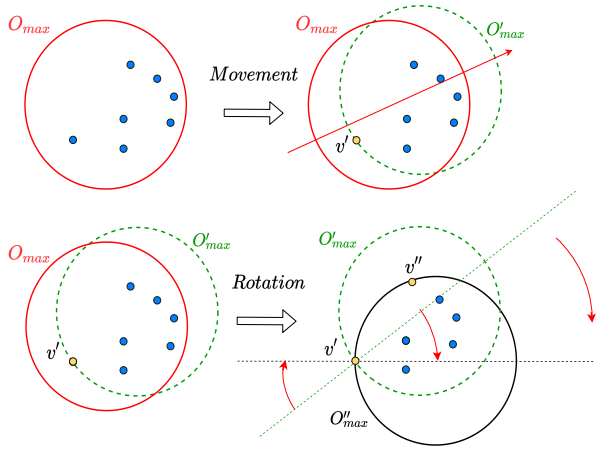

Fig. 6: An instance of Movement and Rotation.

$\Lambda_{max} \leq \Lambda_m$. Since Λ_{max} is the global maximum utility gain at time unit t, we have $\Lambda_{max} \geq \Lambda_m$, hence $\Lambda_m = \Lambda_{max}$. □

Lemma 2: If $|S_{max}| \geq 2$, there exists a location $m \in \mathcal{M}_2$, with the utility gain $\Lambda_m = \Lambda_{max}$ at time unit t.

Proof The claim can be shown as long as a location $m \in \mathcal{M}_2$ with $\Lambda_m = \Lambda_{max}$ can be found. In the following, we show how to identify location m from $\mathcal{M}_2$.

We first find a disk O_{max} on the ground centered at the projection of p_{max} with radius $r = \sqrt{R^2 - H^2}$, where sensors covered by O_{max} (including sensors inside the disk area and sensors on its circumference) are the same as sensors contained in S_{max}. If the number of sensors on the circumference of disk O_{max} is no less than 2, we can obtain a location $m = p_{max}$; otherwise, we find location m by performing operations: *Movement* and *Rotation*. (For an example, see Figure 6.)

- *Movement:* If no sensor is on the circumference of disk O_{max}, move the disk in an arbitrary direction until a sensor sits on its circumference.

Denote by O'_{max} and p'_{max} the disk and its center after the `Movement` operation. Note that, it is very likely to have more than one sensor on the circumference of disk O'_{max}. We can identify the location $m = p'_{max}$ if there are at least 2 sensors on the circumference of O'_{max}. Otherwise, we proceed with the `Rotation` operation as follows.

- *Rotation:* Denote by v' the location of the only one sensor on the circumference of disk O'_{max}. Rotate disk O'_{max} about the pivot point v' in either clockwise or anti-clockwise direction until a sensor (other than v') is on its circumference.

Denoting by O''_{max} and p''_{max} the disk and its center after the `Rotation` operation, the location $m = p''_{max}$ can be obtained. It is possible that there are more than two sensors sitting on the circumference of disk O''_{max}.

We conclude that the location m is either p_{max}, p'_{max}, or p''_{max}. Consequently, we find a disk O_{max}, O'_{max} or O''_{max} centered at m with no less than two sensors sitting on its circumference. Let v_a and v_b be any two sensors on the circumference of the disk. By Step 5 to Step 10 in `Algorithm 1`, one or two locations can be identified based on (v_a, v_b), which must contain m. This is due to the fact that with a fixed radius and two nodes on the circumference, at most two circles can be formed. We thus have $m \in \mathcal{M}_2$.

Having identified the location m, we now show that the sensors covered by O_{max} do not change when applying both the `Movement` and `Rotation` operations.

`Movement` starts when no sensor is on the circumference of O_{max}, and ends at O'_{max} when the first sensor is on its the circumference. Let v_a be a sensor on the circumference of O'_{max}. Before v_a is on the circumference, no sensor covered by O_{max} (sensors inside or on the circumference of O_{max}) leaves out of O_{max} during the `Movement` operation. Otherwise, this conflicts with the fact that sensor v_a is the first sensor on the circumference. Denote by Λ'_{max} the utility gain of sensors covered by O'_{max} at time unit t. We then have $\Lambda'_{max} \geq \Lambda_{max}$. Since Λ_{max} is the maximum utility gain at time t over the UAV serving area, i.e., $\Lambda_{max} \geq \Lambda'_{max}$, we have $\Lambda_{max} = \Lambda'_{max}$.

`Rotation` starts with O'_{max} when only one sensor v' is on its circumference, and ends at O''_{max} when the first sensor (other than v') is on the circumference of O''_{max}. Let Λ''_{max} be the utility gain of sensors covered by O''_{max}. Then $\Lambda''_{max} = \Lambda'_{max}$ can be shown similar to the `Movement` operation.

Thus, `Movement` and `Rotation` operations do not change the sensors covered by disk O_{max}. As a result, there must exist a location $m \in \mathcal{M}_2$ with $\Lambda_m = \Lambda_{max}$ if $|S_{max}| \geq 2$. □

Theorem 2: The hovering location set $\mathcal{M}$ generated by `Algorithm 1` is an $\mathbb{M}$-Set by the properties in Definition 3.

Proof Following Lemma 1 and Lemma 2, there always exists a location $m \in \mathcal{M}$ with the maximum utility gain compared with other locations in the UAV serving area at any time unit. From Step 3 to Step 4, and from Step 5 to Step 10 in `Algorithm 1`, there are at most $|\mathcal{V}|$ and $|\mathcal{V}| \cdot (|\mathcal{V}| - 1)$ locations identified, respectively. The set $\mathcal{M}$ thus is a finite set, and theorem follows. □

We now analyze the approximation ratio of the proposed `Algorithm 2`. A location $l_t = m_{j^*}$ with the maximum utility gain is selected from $\mathbb{M}$-Set at time unit t by Step 6. Denote by z_t the increment of the total utility gain by selecting $l_t = m_{j^*}$, i.e., $z_t = \Lambda_{j^*}(t)$. Denote by Z_t the total utility gain by selecting $l_1, l_2, ..., l_t$ so far, i.e.,$Z_t = \sum_{x=1}^{t} z_x$. Let OPT and g_t denote the total utility gain of the optimal solution, and the difference between OPT and Z_t, i.e., $g_t = OPT - Z_t$.

Lemma 3:

(i) $z_{t+1} \geq \frac{g_t}{\Gamma}$, for $0 \leq t \leq \Gamma - 1$, where$z_0 = Z_0 = 0$, and $g_0 = OPT$.

(ii) $g_{t+1} \leq (1 - \frac{1}{\Gamma})^{t+1} \cdot OPT$, for $0 \leq t \leq \Gamma - 1$.

Proof (i) Recall that g_t is the difference of the total utility gain between OPT and Z_t. By the Pigeonhole Principle, one of the Γ selections in the optimal solution must have at least $\frac{g_t}{\Gamma}$ amount of utility gain. Note that the utility gain at l_{t+1} at time

Authorized licensed use limited to: CITY UNIV OF HONG KONG. Downloaded on July 29,2021 at 08:11:05 UTC from IEEE Xplore. Restrictions apply.

$t+1$ is no less than the utility gain at other locations in $\mathcal{M}$, which always contains the location with the global maximum utility gain by Theorem 2. Therefore, we have that z_{t+1} is the global maximum utility gain at time unit t, i.e., $z_{t+1} \geq \frac{g_t}{\Gamma}$ for $0 \leq t \leq \Gamma - 1$.

(ii) We show the claim by induction. For the base case $t = 0$, since $g_t = OPT - Z_t$, we have

$$g_1 \leq OPT - Z_1 = OPT - z_1 \quad (18)$$
$$\leq OPT - \frac{g_0}{\Gamma} \quad \text{by Lemma 3(i)} \quad (19)$$
$$= OPT - \frac{OPT}{\Gamma} = (1 - \frac{1}{\Gamma}) \cdot OPT \quad (20)$$

Assuming that $g_t \leq (1 - \frac{1}{\Gamma})^t \cdot OPT$, we show as follows $g_{t+1} \leq (1 - \frac{1}{\Gamma})^{t+1} \cdot OPT$.

$$g_{t+1} = g_t - z_{t+1} \leq g_t - \frac{g_t}{\Gamma} \quad \text{by Lemma 3(i)} \quad (21)$$
$$= g_t(1 - \frac{1}{\Gamma}) \quad (22)$$
$$\leq (1 - \frac{1}{\Gamma})^{t+1} \cdot OPT, \text{ by induction hypothesis} \quad (23)$$

□

Theorem 3: The approximation ratio of `Algorithm 2` for the Utility Maximization Problem is $(1 - \frac{1}{e})$.

Proof By Lemma 3, $g_\Gamma \leq (1 - \frac{1}{\Gamma})^\Gamma \cdot OPT$. Since $(1 - \frac{1}{\Gamma})^\Gamma \approx \frac{1}{e}$, we have $g_\Gamma \leq \frac{OPT}{e}$. Thus,

$$Z_\Gamma = OPT - g_\Gamma$$
$$\geq OPT - \frac{OPT}{e}$$
$$= OPT(1 - \frac{1}{e}). \quad (24)$$

Hence, the proof follows. □

V. Performance Evaluation

In this section, we evaluate the performance of the proposed algorithms by simulation experiments, and investigate the impacts of important parameters on the algorithm performance.

A. Experimental Setting

We consider a UAV-enabled WSN deployed in an area with $1,000 \times 1,000$ square meters, where sensors are randomly distributed [25]. The data transmission range and bandwidth of each sensor v_i are 150 meters and 1 Mbps, respectively [28]. The utility margin function of each sensor v_i is generated by $f_i(t) = \alpha \times \frac{1}{t^\beta + \gamma}$, where $\alpha \in [1,\ 100]$, $\beta \in [0.1,\ 1]$ and $\gamma \in [1,\ 2]$ are constants. We employ a UAV for data collection, with the hovering altitude $H = 120$ meters. The hovering budget of the UAV is set as $\Gamma = 1,800$ seconds [25], where the length of each time unit is one second. These parameters are adopted in the default setting, unless otherwise specified.

B. Comparison Heuristics

Since the UMP is a new problem, existing algorithms in the literature can not be directly compared with it. To evaluate the performance of `Algorithm 2` for the UMP, we propose the following four baseline heuristics.

D-Gre. It first discretizes the monitoring area into square regions with a side length of 10 meters. It then adopts a *Greedy* algorithm for generating a UAV data collection tour, i.e., a region d_{max} with the maximum utility is selected iteratively, and the UAV hovers at a random location p_{max} within the region d_{max} until all data from sensors in S_{max} are collected. This procedure continues until the accumulative hovering time of the UAV reaches the budget.

R-Gre. It first identifies 100 locations randomly from the UAV serving area as potential hovering locations. It then adopts the *Greedy* algorithm to iteratively select a location p_{max} with the maximum utility from the 100 identified locations.

S-Gre. The projection (x_i, y_i, H) of each sensor v_i at altitude H is regarded as a potential hovering location for the UAV, with *Greedy* adopted for forming a UAV data collection tour.

S-N. The projection of each sensor v_i at altitude H is recognized as a potential hovering location for the UAV. From these identified locations, p_{max_1} with the maximum utility is selected, where the UAV will collect all data from the sensors in S_{max_1}. Then p_{max_2} is selected from the neighbors of p_{max_1} (no larger than 180 meters away from p_{max_1}) where data are also fully collected. The procedure continues until the accumulative hovering time of the UAV reaches the budget.

The value plotted in each figure is the mean of the results out of 50 WSN instances with the same size. The running time of all mentioned simulations is obtained from a desktop with 4.0 GHz Intel Core i7 CPU and 32 GB RAM.

C. Experimental Results

We first evaluate the performance of `Algorithm 1` that aims to identify potential hovering locations for the UAV in order to maximize the total utility in the end. Here we propose grid-based four heuristics `D-10`, `D-50`, `D-100` and `D-200` for comparison purposes, which divide the monitoring area of sensors into numbers of square regions with side lengths 10, 50, 100 and 200 meters respectively and adopt Step 2 to Step 17 of `Algorithm 2` for generating a UAV data collection tour. We evaluate the performance of `Algorithm 1` by comparing the simulation results of `Algorithm 2` (denoted by `Alg02`) against the mentioned four heuristics, where the only difference between them is the set of identified potential hovering locations. The square sizes of the simulated networks vary from 600 meters to 1,500 meters, with 400 sensors randomly deployed.

Fig. 7(a) demonstrates that the data collection utility of `Alg02` significantly outperforms other discretization-based heuristics. With increasing network area, the data collection utility of all such algorithms declines, due to the fact that fewer sensors are located in the data reception range of the UAV in sparser networks. Fig. 7(b) plots the running time of `Alg02`,

Authorized licensed use limited to: CITY UNIV OF HONG KONG. Downloaded on July 29,2021 at 08:11:05 UTC from IEEE Xplore. Restrictions apply.

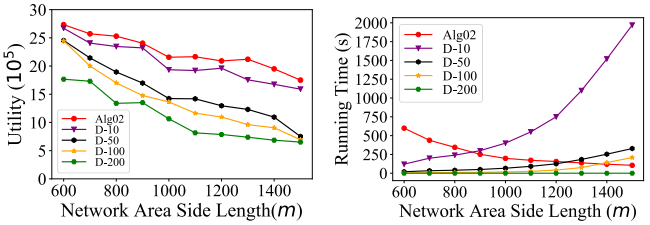

(a) (b)

Fig. 7: Performance of `Alg02`, `D-10`, `D-50`, `D-100` and `D-200` in WSNs by varying the side length of the network area from 600 meters to $1,500$ meters.

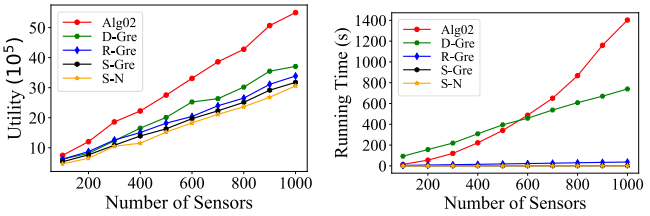

(a) (b)

Fig. 8: Performance of `Alg02`, `D-Gre`, `R-Gre` and `S-Gre`, `S-N` in WSNs consisting of sensors from 100 to $1,000$.

which decreases with the size of the network area, while it increases rapidly for other discretization-based heuristics.

Next we compare the performance of `Algorithm 2` with the aforementioned four heuristics `D-Gre`, `R-Gre`, `S-Gre` and `S-N`, by varying the number of sensors from 100 to $1,000$. Fig.8(a) depicts that `Alg02` significantly outperforms the four mentioned heuristics. In particular, the utility delivered by `Alg02` is approximately 149% of that by `D-Gre`, and 170% of the utilities by other heuristics. Fig.8(b) plots the running time of the proposed algorithms.

D. Impacts of Parameters on the Performance

We investigate the impacts of the UAV hovering budget and the data transmission range of sensors on the performance of the algorithms in sensor networks of 400 sensors.

We first study the impact of the UAV hovering budget on the performance of the mentioned algorithms, by varying the UAV hovering budget from $1,000$ to $10,000$ time units. Fig. 9(a) shows that the utilities of different algorithms rapidly grow with the increase on the UAV hovering budget. It can be seen that `Alg02` significantly outperforms the other heuristics in all cases. Fig. 9(b) demonstrates that the running time of `Alg02` increases with that of the UAV hovering budget.

We also investigate the impact of the transmission range of sensors on the performance of the mentioned algorithms. Note that the data transmission range of sensors should be no less than the hovering altitude of the UAV; otherwise, the transmitted data from sensors cannot be collected by the UAV. We evaluate the performance of the proposed algorithms by varying the data transmission range of sensors from 140 meters to 200 meters. It can be seen from Fig. 10(a) that the utilities

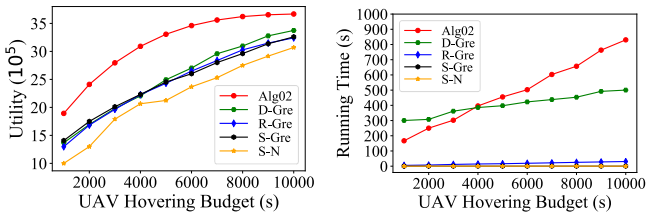

(a) (b)

Fig. 9: Performance of `Alg02`, `D-Gre`, `R-Gre` and `S-Gre`, `S-N` in WSNs with UAV hovering budgets from $1,000$ to $10,000$ seconds.

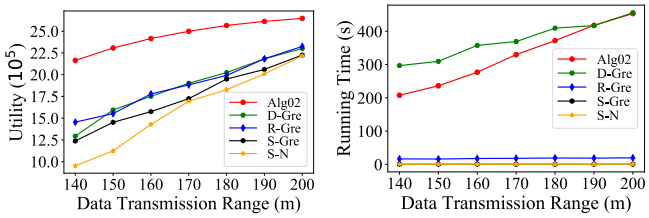

(a) (b)

Fig. 10: Performance of `Alg02`, `D-Gre`, `R-Gre` and `S-Gre`, `S-N` in WSNs by varying the data transmission range of sensors from 140 meters to 200 meters.

delivered by different algorithms grow with the increase on the data transmission range, due to the fact that more sensors can be covered by the UAV. Fig. 10(b) plots the running times of different algorithms.

VI. Conclusion

In this paper, we studied the maximization of data collection utility in a UAV-enabled WSN under the one-to-many data collection scheme, where the UAV hovering location positioning and the data collection utility need to be jointly considered. To this end, we first formulated the data collection utility maximization problem (UMP). We then devised an efficient algorithm to identify a finite set of potential hovering locations for the UAV that improves the data collection utility significantly. we further proposed an approximation algorithm for UMP with an approximation ratio of $(1 - \frac{1}{e})$. Finally, we evaluated the proposed algorithm through simulation study and compared with four baseline greedy heuristics. Simulation results demonstrate that the proposed algorithm significantly outperforms the greedy heuristics. As part of future work, we plan to take into consideration the energy consumption of the UAV during the tour for data collection utility maximization in wireless sensor networks.

Acknowledgements

The work of Mengyu Chen and Weifa Liang was supported by the Australian Research Council Discovery Projects DP200101985 and DP210103002. The work of Sajal K. Das is supported by the NSF grants CNS-2008878, SCC-IRG-1952045, and PPoSS-1725755.

Authorized licensed use limited to: CITY UNIV OF HONG KONG. Downloaded on July 29,2021 at 08:11:05 UTC from IEEE Xplore. Restrictions apply.

REFERENCES

[1] A. Ometov, P. Masek, L. Malina, R. Florea, J. Hosek, S. Andreev, J. Hajny, J. Niutanen and Y. Koucheryavy. "Feasibility characterization of cryptographic primitives for constrained (wearable) IoT devices". In *Proceedings of IEEE International Conference on Pervasive Computing and Communications Workshops* (PerCom Workshops), pp. 1–6, 2016.

[2] F. Gu, J. Niu, S. K. Das, Z. He and X. Jin. "Detecting breathing frequency and maintaining a proper running rhythm". *Pervasive and Mobile Computing*, vol 42, 2017.

[3] A. Dorri, S. S. Kanhere, R. Jurdak and P. Gauravaram. "Blockchain for IoT security and privacy: The case study of a smart home". *Proceedings of IEEE International Conference on Pervasive Computing and Communications Workshops*, pp. 618–623, 2017.

[4] S. Roy, N. Ghosh and S. K. Das. "bioSmartSense: A Bio-inspired Data Collection Framework for Energy-efficient, QoI-aware Smart City Applications". *Proceedings of IEEE International Conference on Pervasive Computing and Communications* (PerCom), pp. 1–10, IEEE, 2019.

[5] R. Satyaki, N. Ghosh, and S. K. Das. "bioSmartSense+: A bio-inspired probabilistic data collection framework for priority-based event reporting in IoT environments". *Pervasive and Mobile Computing*, vol.67, 2020.

[6] C. Cabrera, A. Palade, G. White and S. Clarke. "An Urban-driven Service Request Management Model". *Proc. IEEE International Conf. on Pervasive Computing and Communications* (PerCom), pp. 1–7, 2020.

[7] A. Ghosal, S. Halder, and S. K. Das. "Distributed on-demand clustering algorithm for lifetime optimization in wireless sensor networks". *Journal of Parallel and Distributed Computing*, vol. 141, 2020.

[8] W. Choi, G. Ghidini, and S. K. Das. "A novel framework for energy-efficient data gathering with random coverage in wireless sensor networks". *ACM Transactions on Sensor Networks*, vol.8, no.4, 2012.

[9] M. Di Francesco, S. K. Das, and G. Anastasi. "Data Collection in Wireless Sensor Networks with Mobile Elements: A Survey". *ACM Transactions on Sensor Networks* (TOSN), vol.8, no.1, 2011.

[10] S. Gao, H. Zhang, and S. K. Das "Efficient Data Collection in Wireless Sensor Networks with Path-Constrained Mobile Sinks". *IEEE Transactions on Mobile Computing*, vol.10, 2011.

[11] J. Wang, Y. Liu, and S. K. Das. "Energy Efficient Data Gathering in Wireless Sensor Networks with Asynchronous Sampling". *ACM Transactions on Sensor Networks* (TOSN), vol.6, no.3, 2010.

[12] A. Navarra, C. M. Pinotti, M. Di Francesco, and S. K. Das. "Interference-free Scheduling with Minimum Latency in Cluster-based Wireless Sensor Networks". *Wireless Networks*, vol.21, no.7, 2015.

[13] S. K. A. Imon, A. Khan, M. Di Francesco, and S. K. Das "Energy-Efficient Randomized Switching for Maximizing Lifetime in Tree-based Wireless Sensor Networks". *IEEE/ACM Transactions on Networking*, vol. 23, No. 5, 1401-1415, Oct 2015.

[14] M. Chen, W. Liang, and J. Li. "Energy-Efficient Data Collection Maximization for UAV-Assisted Wireless Sensor Networks". To appear in *Proceedings of IEEE Wireless Communications and Networking Conference* (WCNC), 2021.

[15] M. Samir, S. Sharafeddine, C. M. Assi, T. M. Nguyen and A. Ghrayeb. "UAV Trajectory Planning for Data Collection from Time-Constrained IoT Devices". *IEEE Transactions on Wireless Communications*, vol. 19, no. 1, pp. 34–46. 2020.

[16] Y. Liang, W. Xu, W. Liang, J. Peng, X. Jia, Y. Zhou, and L. Duan. "Nonredundant information collection in rescue applications via an energy-constrained uav". *IEEE Internet of Things Journal*, vol. 6, no. 2, pp. 2945–2958, 2018.

[17] A. Khochare, Y. Simmhan, F. B. Sorbelli, and S. K. Das. "Heuristic Algorithms for Co-scheduling of Edge Analytics and Routes for UAV Fleet Missions". To appear in *Proceedings of IEEE International Conference on Computer Communications* (INFOCOM), 2021.

[18] Y. Li, W. Liang, W. Xu, and X. Jia. "Data collection of IoT devices using an energy-constrained UAV". *Proceedings of IEEE International Parallel and Distributed Processing Symposium* (IPDPS), pp.644–653, 2020.

[19] J. Liu, X. Wang, B. Bai and H. Dai. "Age-optimal trajectory planning for UAV-assisted data collection". In *Proceedings of IEEE International Conference on Computer Communications Workshops* (INFOCOM WKSHPS), pp. 553–558, IEEE, 2018.

[20] J. Zhang, Z. Li, W. Xu, J. Peng, W. Liang, Z. Xu, X. Ren, and X. Jia. "Minimizing the number of deployed UAVs for delay-bounded data collection of IoT devices". To appear in *Proceedings of IEEE International Conference on Computer Communications* (INFOCOM), IEEE, 2021.

[21] A. Trotta, M. D. Felice, L. Bononi, E. Natalizio, L. Perilli, E. F. Scarselli, T. S. Cinotti and R. Canegallo. "BEE-DRONES: Energy-efficient Data Collection on Wake-Up Radio-based Wireless Sensor Networks". *Proceedings of IEEE International Conference on Computer Communications Workshops* (INFOCOM WKSHPS), pp: 547–553, 2019.

[22] M. Mozaffari, W. Saad, M. Bennis, and M. Debbah. "Mobile internet of things: Can uavs provide an energy-efficient mobile architecture?" *Proceedings of IEEE global communications conference (GLOBECOM)*, pp. 1–6, 2016.

[23] A. Farajzadeh, O. Ercetin and H. Yanikomeroglu. "UAV Data Collection Over NOMA Backscatter Networks: UAV Altitude and Trajectory Optimization". *Proceedings of IEEE International Conference on Communications (ICC)*, pp. 1–7, 2019.

[24] C. Caillouet, F. Giroire and T. Razafindralambo. "Optimization of mobile sensor coverage with UAVs". *Proceedings of IEEE International Conference on Computer Communications Workshops* (INFOCOM WKSHPS), pp. 622–627, 2018.

[25] M. Chen, W. Liang and Y. Li "Data collection maximization for UAV-enabled wireless sensor networks". *Proceedings of the International Conference on Computer Communications and Networks* (ICCCN), pp.1–9, 2020.

[26] M. Charikar, S. Khuller, D.M. Mount, G. Narasimhan. "Algorithms for facility location problems with outliers". *ACM Symposium on Discrete Algorithms*, vol. 1, pp. 642–651. 2001.

[27] B. Xiao, J. Cao, Q. Zhuge, Y. He and E. H. -M. Sha. "Approximation algorithms design for disk partial covering problem". *Proceedings of 7th International Symposium on Parallel Architectures, Algorithms and Networks* (ISPAN), pp. 104–109, 2004.

[28] J. Theunissen, H. Xu, R. Y. Zhong and X. Xu. "Smart AGV system for manufacturing shopfloor in the context of Industry 4.0". *Proceedings of 25th International Conference on Mechatronics and Machine Vision in Practice* (M2VIP), pp. 1–6, 2018.

Authorized licensed use limited to: CITY UNIV OF HONG KONG. Downloaded on July 29,2021 at 08:11:05 UTC from IEEE Xplore. Restrictions apply.